

Polariton quantum blockade in a photonic dot

A. Verger,¹ C. Ciuti,^{1,*} and I. Carusotto²

¹*Laboratoire Pierre Aigrain, Ecole Normale Supérieure, 24, rue Lhomond, 75005 Paris, France*

²*BEC-CNR-INFN and Dipartimento di Fisica, Università di Trento, I-38050 Povo, Italy*

(Dated: November 1, 2018)

We investigate the quantum nonlinear dynamics of a resonantly excited photonic quantum dot embedding a quantum well in the strong exciton-photon coupling regime. Within a master equation approach, we study the polariton quantum blockade and the generation of single photon states due to polariton-polariton interactions as a function of the photonic dot geometry, spectral linewidths and energy detuning between quantum well exciton and confined photon mode. The second order coherence function $g^{(2)}(t, t')$ is calculated for both continuous wave and pulsed excitations.

Several recent developments in the field of quantum information [1] and quantum communication [2] are based on light beams with strongly non-classical properties. Many techniques have been developed to obtain such beams, using, e.g., parametric down-conversion processes in bulk nonlinear crystals [1], colored centers in diamond [3] or by taking advantage of semiconductor electronic quantum nanodots [4, 5, 6]. These are a sort of artificial two-level atoms, which are able to absorb and diffuse one quantum of radiation at a time, so that the emitted light shows strong antibunching properties and a train of single-photon pulses can be obtained under pulsed excitation. However, the use of self-organized quantum nanodots requires non-trivial nanotechnology to control the emission frequency and spatial position[7]. In addition to this, the coupling to the photon mode is far from optimal, due to the large mismatch between the spatial size of the electron nanodot and of the photonic mode, as attested by the intrinsically small vacuum Rabi energy[8, 9] (typically a fraction of a meV).

Quantum wells strongly coupled to planar microcavities combine strong nonlinearities due to exciton-exciton interactions with an efficient coupling to radiation. In particular, their use as parametric amplifiers and oscillators working at low pump intensities appears promising [10, 11, 12, 13, 14, 15]. Very recently, lithographic techniques have been developed to create high quality photonic dots able to confine the photon without spoiling the strong-coupling with the quantum well exciton. In this way, polaritons result confined in all three dimensions with large vacuum Rabi splittings (several meVs) [16, 17].

In this Letter, we discuss a proposal of a single photon source based on such a kind of polariton quantum dot as the active medium. If the photonic confinement volume is small enough, the presence of just one polariton can block the resonant injection of an additional polariton, because the polariton-polariton interaction can shift the resonance frequency by an amount of the order of the linewidth or even larger. The emitted light is therefore strongly anti-bunched. If a pulsed pump is used, this

may result in a single-photon light source. The quantum polariton blockade effect here considered is reminiscent of the one proposed for atomic matter waves [18] and, more closely, for photons in cavities with a nonlinear atomic medium [19, 20]. An important advantage of using polaritons comes from the strong exciton-exciton interactions, while the photonic component guarantees an efficient and fast coupling to the radiative modes outside the cavity where the emission takes place.

The quantum emission properties of the proposed system are quantitatively studied by means of the master equation for the coupled exciton and cavity photon fields including losses. In particular, we have studied the behavior of the second-order coherence function $g^{(2)}$ as a function of the relevant physical parameters, and we have identified the regimes where the antibunching is most effective. These results are then used to characterize the emission in the presence of a pulsed source, which is shown to provide a train of single-photon pulses.

We start our theoretical treatment by recalling the quantum Hamiltonian model [13, 14, 15] describing a quantum well exciton strongly coupled to a planar microcavity photon mode, namely

$$\begin{aligned}
 H = & \int d\vec{x} \sum_{i,j \in \{X,C\}} \hat{\Psi}_i^\dagger(\vec{x}) h_{i,j}^0(-i\nabla) \hat{\Psi}_j(\vec{x}) \\
 & + \frac{\hbar\kappa}{2} \int d\vec{x} \hat{\Psi}_X^\dagger(\vec{x}) \hat{\Psi}_X^\dagger(\vec{x}) \hat{\Psi}_X(\vec{x}) \hat{\Psi}_X(\vec{x}) \\
 & - \frac{\hbar\Omega_R}{n_{sat}} \int d\vec{x} \hat{\Psi}_C^\dagger(\vec{x}) \hat{\Psi}_X^\dagger(\vec{x}) \hat{\Psi}_X(\vec{x}) \hat{\Psi}_C(\vec{x}) + h.c \\
 & + \int d\vec{x} \hbar F_p(\vec{x}, t) e^{-i\omega_p t} \hat{\Psi}_C^\dagger(\vec{x}) + h.c, \quad (1)
 \end{aligned}$$

where the field operators $\hat{\Psi}_{X,C}$ describe excitons (X) and cavity photons (C). These operators depend on the in-plane position wavevector \vec{x} , which is perpendicular to the growth direction z . They satisfy Bose commutation rules $[\hat{\Psi}_i(\vec{x}), \hat{\Psi}_j^\dagger(\vec{x}')] = \delta^2(\vec{x} - \vec{x}')\delta_{i,j}$. The linear term, including the exciton and planar microcavity photon kinetic energy (the motion along z is quantized), reads

$$h^0(-i\nabla) = \hbar \begin{pmatrix} \omega_X(-i\nabla) & \Omega_R \\ \Omega_R & \omega_C(-i\nabla) + V_C(\vec{x}) \end{pmatrix}, \quad (2)$$

*Electronic address: ciuti@lpa.ens.fr

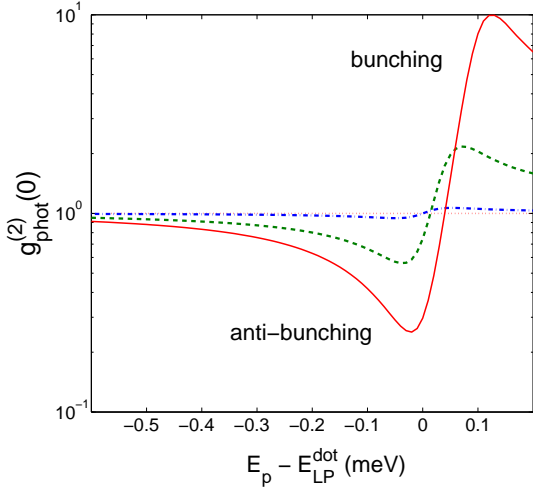


FIG. 1: Second order coherence function $g^{(2)}(0)$ versus pump detuning $\hbar\omega_p - \hbar\omega_{LP}^{\text{dot}}$ (meV) for three different cavity-exciton detunings. Solid, dashed, dotted-dashed line: $\hbar(\omega_C^{\text{dot}} - \omega_X) = 5, 0, -5$ meV. Parameters: $\hbar\omega_{nl} = 0.4$ meV, $\hbar\gamma_X = \hbar\gamma_C = 0.1$ meV and continuous wave excitation field $\hbar\mathcal{F}_0 = 10^{-2}$ meV.

where the exciton-photon coupling, responsible for the appearance of the polariton eigenmodes, is quantified by the vacuum Rabi frequency Ω_R . $V_C(\vec{x})$ describes the photonic dot confining potential due to the lithographic patterning. Two contributions are responsible for the polariton nonlinearities, namely the exciton-exciton interaction (modeled through a repulsive contact interaction potential with strength $\hbar\kappa$) and the anharmonic exciton-photon coupling (depending on the exciton oscillator strength saturation density n_{sat}). Finally, $F_p(\vec{x}, t)$ describes the applied pump field with frequency ω_p .

The photon field operator can be expanded in terms of the confined modes in the photonic dot, namely $\hat{\Psi}_C(\vec{x}) = \sum_j \phi_{C,j}(\vec{x}) \hat{a}_j$, where $\phi_{C,j}$ is the normalized wavefunction of the j -th mode of energy $\hbar\omega_{C,j}^{\text{dot}}$, while \hat{a}_j is the corresponding annihilation operator. Since the exciton kinetic energy is negligible compared to the photonic one (i.e., the exciton mass can be approximated as infinite), it is convenient to use the same basis to expand the exciton operator as $\hat{\Psi}_X(\vec{x}) = \sum_j \phi_{C,j}(\vec{x}) \hat{b}_j$, where \hat{b}_j is the corresponding exciton annihilation operator. In fact, it can be easily seen from Eq. (2) that each photon mode is coupled only to the exciton mode with the same spatial wavefunction, implying that the polariton eigenmodes have the same spatial wavefunction as the photonic dot modes. In the following, we will be interested in studying the dynamics of the fundamental photonic mode confined in the photonic dot, when this is close to resonance with the exciton level. In the case of a strong photonic confinement, the energy spacing between confined photon modes can become much larger than the mode spectral linewidth and the energy detuning between the quantum well exciton resonance and the considered photon

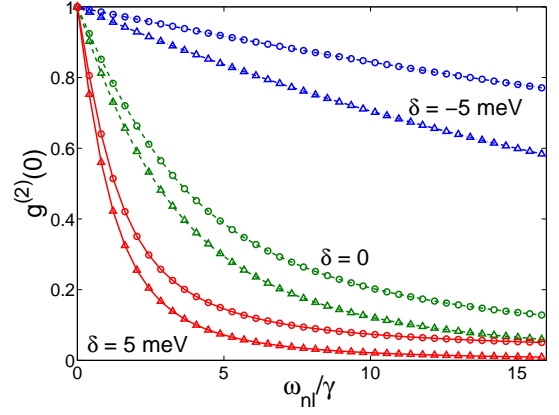


FIG. 2: Second order coherence function $g^{(2)}(0)$ for the photon (circles) and exciton (triangles) as a function of the normalized nonlinear coefficient ω_{nl}/γ for three different values of $\delta = \hbar(\omega_C^{\text{dot}} - \omega_X)$. Parameters: $\hbar\gamma_X = \hbar\gamma_C = 0.1$ meV and $\omega_{LP}^{\text{dot}} = \omega_p$.

mode. In this limit and for quasi-resonant excitation, we can safely simplify our quantum description by retaining in the Hamiltonian only the fundamental photonic dot mode of energy $\hbar\omega_C^{\text{dot}}$ and the exciton mode having the same spatial wavefunction $\phi_C(\vec{x})$. Thus, in the following, we will consider the following effective Hamiltonian:

$$\begin{aligned}
 H_{eff} = & \hbar\omega_X b^\dagger b + \hbar\omega_C^{\text{dot}} a^\dagger a + \hbar\Omega_R b^\dagger a + \hbar\Omega_R b a^\dagger \\
 & + \frac{\hbar\omega_{nl}}{2} b^\dagger b^\dagger b b - \alpha_{sat} \hbar\Omega_R b^\dagger b^\dagger a b - \alpha_{sat} \hbar\Omega_R a^\dagger b^\dagger b b \\
 & + \hbar\mathcal{F}_0(t) e^{-i\omega_p t} a^\dagger + \hbar\mathcal{F}_0^*(t) e^{i\omega_p t} a, \quad (3)
 \end{aligned}$$

where a and b are the annihilation operators of the considered photonic dot and exciton mode respectively. The parameters involved in the effective Hamiltonian are the applied laser amplitude $\mathcal{F}_0(t) = \int d\vec{x} F_p(\vec{x}, t) \phi_C^*(\vec{x})$, while $\alpha_{sat} = \frac{1}{n_{sat}} \int d\vec{x} |\phi_C(\vec{x})|^4$ and $\omega_{nl} = \kappa \int d\vec{x} |\phi_C(\vec{x})|^4$ are the effective nonlinear coefficients. The saturation coefficient α_{sat} will be neglected in the numerical solution because $\frac{\alpha_{sat} \hbar\Omega_R}{\hbar\omega_{nl}/2} = \frac{2\Omega_R}{n_{sat}\kappa} \ll 1$ for typical III-V microcavity parameters[13].

To give the dependance of the nonlinear coefficient ω_{nl} on the photonic dot confinement, we have considered two simple geometries with infinite confinement barriers. In the case of a squared dot, the normalized wavefunction is $\phi(x, y) = \frac{2}{L} \sin(\frac{\pi}{L}x) \sin(\frac{\pi}{L}y)$ where L is the lateral size. In the cylindrical case, $\phi(r) = \frac{1.087}{R} J_0(2.405 r/R)$ where R is the radius of the cylinder and J_0 the zeroth order Bessel function. The values of the geometric coefficients are $\int_{square} d\vec{x} |\phi_C(\vec{x})|^4 = 2.25/L^2$, and $\int_{cylinder} d\vec{x} |\phi_C(\vec{x})|^4 = 2.67/(2R)^2$, showing the inverse proportionality between ω_{nl} and the lateral area of the photonic mode. In order to study the quantum dynamics, it is convenient to work in the rotating frame described by the operator $R = e^{i(\omega_p t (a^\dagger a + b^\dagger b))}$. The rotating frame

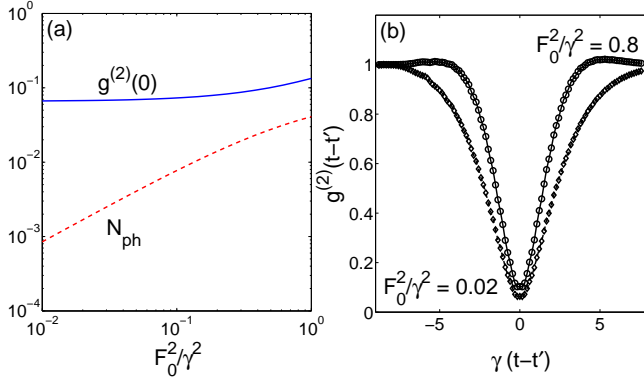


FIG. 3: (a) Second order coherence function $g_{phot}^{(2)}(0)$ (solid line) and intracavity photon population (dotted line) inside the dot as a function of pump power in the continuous wave regime. (b) Second order coherence function $g_{phot}^{(2)}(t, t')$ at a fixed t' as a function of time for two different pump powers. Parameters: $\hbar(\omega_C^{dot} - \omega_X) = 5$ meV, $\hbar\omega_{nl} = 1$ meV, $\hbar\gamma_X = \hbar\gamma_C = 0.1$ meV.

Hamiltonian is:

$$\begin{aligned} \tilde{H}_{eff} = & \hbar\Delta\omega_X b^\dagger b + \hbar\Delta\omega_C a^\dagger a + \hbar\Omega_R b^\dagger a + \hbar\Omega_R b a^\dagger \\ & + \frac{\hbar\omega_{nl}}{2} b^\dagger b^\dagger b b + \hbar\mathcal{F}_0(t) a^\dagger + \hbar\mathcal{F}_0^*(t) a, \end{aligned} \quad (4)$$

$$\begin{aligned} g_{phot}^{(2)}(t, t') &= \frac{G_{phot}^{(2)}(t, t')}{N_{ph}(t)N_{ph}(t')} = \frac{Tr(a \mathcal{U}_{t,t'} [a\tilde{\rho}(t')a^\dagger] a^\dagger)}{Tr(a\tilde{\rho}(t)a^\dagger)Tr(a\tilde{\rho}(t')a^\dagger)} = \frac{\sum_{m,n} m\theta_{n,m,n,m}(t, t')}{\sum_{m,n} m\tilde{\rho}_{n,m,n,m}(t) \sum_{m,n} m\tilde{\rho}_{n,m,n,m}(t')}, \quad \forall t > t' \\ \theta(t, t') &= \mathcal{U}_{t,t'} \left[\sum_{n,m,n',m'} \tilde{\rho}_{n',m',n,m}(t') \sqrt{mm'} |n', m' - 1\rangle \langle n, m - 1| \right], \end{aligned} \quad (7)$$

where $\mathcal{U}_{t,t'}$ is the evolution superoperator associated to the master equation (5).

As we have already discussed, we will consider the case of an applied optical field with frequency ω_p close to the frequency $\omega_{LP}^{dot} = \frac{\omega_C^{dot} + \omega_X}{2} - \sqrt{\Omega_R^2 + \frac{(\omega_C^{dot} - \omega_X)^2}{4}}$ of the fundamental confined polariton mode in the dot. In the case of a continuous wave excitation, we give in Fig. 1 an example of the dependence of the equal-time second-order coherence $g_{phot}^{(2)}(0) \equiv g_{phot}^{(2)}(t, t)$ on the pump detuning $\omega_p - \omega_{LP}^{dot}$ for a given set of parameters. For a pump laser frequency red-detuned or close to resonance with the fundamental polariton resonance, $g_{phot}^{(2)}(0) < 1$, implying sub-poissonian statistics and antibunching. This is the regime where the polariton quantum blockade is working. Indeed, the photon injection is inhibited when only a small number of polaritons are already inside the dot due to the interaction-induced blueshift of the polariton resonance. For large values of ω_{nl}/γ , only one polariton can be present in the dot with a vanishing probability of having two at the same time, implying

where $\Delta\omega_C = \omega_C^{dot} - \omega_p$ and $\Delta\omega_X = \omega_X - \omega_p$ respectively. To describe the quantum dynamics in presence of damping, we have considered the master equation for the density matrix $\rho(t)$:

$$\begin{aligned} \frac{\partial \tilde{\rho}}{\partial t} = & \frac{i}{\hbar} [\tilde{\rho}, \tilde{H}_{eff}] + \gamma_C (a\tilde{\rho}a^\dagger - 1/2(a^\dagger a\tilde{\rho} + \tilde{\rho}a^\dagger a)) \\ & + \gamma_X (b\tilde{\rho}b^\dagger - 1/2(b^\dagger b\tilde{\rho} + \tilde{\rho}b^\dagger b)), \end{aligned} \quad (5)$$

where $\tilde{\rho} = R\rho R^\dagger$, while γ_X and γ_C are the homogeneous broadening of the exciton and photon modes. The master equation can be solved by expanding the density matrix over a Fock basis, namely

$$\tilde{\rho}(t) = \sum_{n'_X, n'_C, n_X, n_C} \tilde{\rho}_{n'_X, n'_C, n_X, n_C}(t) |n'_X, n'_C\rangle \langle n_X, n_C|, \quad (6)$$

where n_X and n_C are the number of excitons and photons respectively. In the following, we will be interested in the two-time second-order coherence function [21], defined as:

$g_{phot}^{(2)}(0) \approx 0$. On the other-hand, for a blue-detuned laser, $g_{phot}^{(2)}(0) > 1$, implying bunching. In Fig. 1, there are three curves corresponding to different detunings $\delta = \hbar(\omega_C^{dot} - \omega_X)$. Since the nonlinearity is due to the excitonic fraction of the polaritonic mode, the photonic antibunching is more pronounced for $\delta > 0$. As shown in Fig. 2, the minimum value of $g_{phot}^{(2)}(0)$ depends critically on the ratio ω_{nl}/γ , where the polariton mode linewidth $\gamma = |X_{LP}|^2\gamma_X + |C_{LP}|^2\gamma_C$, being $|X_{LP}|^2$ and $|C_{LP}|^2$ the excitonic and photonic fractions of the lower polariton mode respectively. Here, for the sake of clarity, we have performed calculations taking $\gamma_X = \gamma_C = \gamma$. The antibunching behavior ($g_{phot}^{(2)}(0) < 1$) starts to be significant when $\omega_{nl}/\gamma \sim 1$. In order to have $\omega_{nl}/\gamma = 1$, with a polariton linewidth $\hbar\gamma = 0.1$ meV and with a realistic nonlinear coefficient [13, 14] $\hbar\kappa = 1.5 \times 10^{-2} (\mu\text{m})^2$ meV (corresponding to an exciton blueshift of 0.15 meV in presence of 10^9 cm^{-2} excitons), a cylindrical dot with diameter $2R = 0.67 \mu\text{m}$ would be required. Reducing further the size allows one to enter the strong quantum blockade regime $\omega_{nl}/\gamma \gg 1$. For example, using

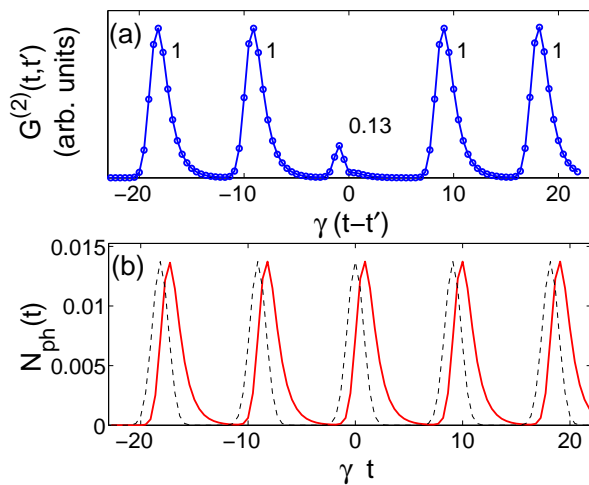


FIG. 4: (a) Second order correlation function $G_{phot}^{(2)}(t, t')$ for $t' = 6$ ps under the excitation of a train of gaussian pulses (pulse duration of 5 ps) separated from each other by 60 ps. The normalized area is indicated for each peak. (b) Corresponding intra-cavity photon population $N_{ph}(t)$. Dotted line: shape of the pump amplitude $\mathcal{F}_0(t)$. Parameters: $\hbar(\omega_C^{dot} - \omega_X) = 5$ meV, $\hbar(\omega_p - \omega_{LP}^{dot}) = 0.05$ meV, $\hbar\omega_{nl} = 1.1$ meV, $|\mathcal{F}_0|^2/\gamma^2 = 0.09$, $\hbar\gamma_X = \hbar\gamma_C = 0.1$ meV, so $1/\gamma = 6.6$ ps.

the same nonlinear coefficient, a square dot with lateral size $L = 0.2 \mu\text{m}$ gives $\omega_{nl}/\gamma = 8.4$. In general, there is slight asymmetry between the photonic and excitonic antibunching ($g_{phot}^{(2)}(0) > g_{exc}^{(2)}(0)$) even at zero detuning. This asymmetry occurs because the nonlinearity is due to the exciton.

Given the current interest for quantum devices, it is useful to characterize the peculiar figures of merit of the single-photon source under consideration. To have an efficient single-photon source, we need to maximize the photon population N_{ph} , keeping the sub-poissonian character strong. To address this issue, in Fig. 3(a) we have plotted $g_{phot}^{(2)}(0)$ and the intra-cavity photon population N_{ph} as a function of the normalized incident intensity $|\mathcal{F}_0|^2/\gamma^2$ of the cw laser. For $|\mathcal{F}_0|^2/\gamma^2 \rightarrow 0$, $g_{phot}^{(2)}(0)$ asymptotically converges to a minimum value, but the population N_{ph} goes to 0. For increasing $|\mathcal{F}_0|^2/\gamma^2$, N_{ph}

increases, but $g_{phot}^{(2)}(0)$ eventually grows up. For the parameters here used, the crossover occurs for $N_{ph} \approx 0.01$. In Fig. 3(b), the dependence of $g_{phot}^{(2)}(t, t')$ on the relative time $t - t'$ is shown for two excitation intensities. It is apparent that the temporal width of the antibunching dip is directly related to the inverse polariton linewidth $1/\gamma$, at least in the limit $|\mathcal{F}_0|^2/\gamma^2 \rightarrow 0$.

Since the polariton quantum blockade effect relies on the resonant character of the excitation, one can wonder whether the effect is robust even in the pulsed excitation regime. In addition to the strong sub-poissonian photon statistics, the efficiency and the repetition rate are the relevant quantities in the pulsed excitation case. We have solved the dynamics using a train of excitation pulses and we have found that by using Fourier-limited pulses with spectral linewidth comparable to the polariton one and a repetition rate $\Gamma \ll \gamma$, the suppression of the two-photon probability approaches the cw case. As an illustrative example, in Fig. 4(a) we show the time-dependent second-order correlation function $G_{phot}^{(2)}(t, t')$. The depletion of the central peak (which would not occur for a source with poissonian statistics, such as an attenuated laser beam) demonstrates the strong single-photon character of the present source even in the pulsed regime. The quantity $\eta = \gamma_C \int_{\Delta T} N_{ph}(t) dt$ (where ΔT is the time interval between two consecutive pulses) represents the averaged number of photons emitted per pulse. As shown in Fig. 4(b), a repetition rate $\Gamma = \gamma/10$ is enough to avoid pulse overlap. The effective quantum bit exchange rate of the present quantum source would be $r = \eta\Gamma$. With respect to the example in Fig. 4(b), we have $\eta \simeq 0.01$, implying $r \simeq 0.1$ GHz.

In conclusion, the present work has predicted the rich quantum nonlinear dynamics of a quantum well exciton transition strongly coupled to a photonic quantum dot mode, showing the potential for the realization of a single-photon source with controllable properties based on the polariton quantum blockade effect.

We thank G. Bastard, B. Deveaud, C. Diederichs, G. Dasbach, O. El Daïf, I. Favero, J.M. Gérard, F. Morier-Genoud, A. Imamoğlu, N. Regnault, J. Tignon for discussions. LPA-ENS is a "Unité Mixte de Recherche Associée au CNRS (UMR 8551) et aux Universités Paris 6 et 7".

[1] D. Bouwmeester, A. Ekert and A. Zeilinger (Eds.), *The physics of quantum information* (Springer-verlag, Berlin, 2000).
 [2] N. Gisin *et al.*, Rev. Mod. Phys. **74**, 145 (2002).
 [3] A. Beveratos *et al.*, Phys. Rev. Lett. **89**, 187901 (2002).
 [4] J.M. Gérard *et al.*, Phys. Rev. Lett. **81**, 1110 (1998).
 [5] P. Michler *et al.*, Science **290**, 2282 (2000).
 [6] J. Kim *et al.*, Nature **397**, 500 (1999); C. Santori *et al.*, Nature **419**, 594 (2002).

[7] A. Badolato *et al.*, Science **308**, 1158 (2005).
 [8] J.P. Reithmaier *et al.*, Nature (London) **432**, 197 (2004); T. Yoshie *et al.*, Nature (London) **432**, 200 (2004); E. Peter *et al.*, Phys. Rev. Lett. **95**, 067401 (2005).
 [9] J.I. Perea, D. Porrás, and C. Tejedor, Phys. Rev. B **70**, 115304 (2004).
 [10] P.G. Savvidis *et al.*, Phys. Rev. Lett. **84**, 1547 (2000).
 [11] C. Ciuti *et al.*, Phys. Rev. B **62**, R4825 (2000).
 [12] M. Saba *et al.*, Nature (London) **414**, 731 (2001).

- [13] J. Baumberg and L. Via (Eds.) Special issue on Microcavities, [Semicond. Sci. Technol. **18**, S279 (2003)].
- [14] B. Deveaud (Ed.), Special issue on the "Physics of semiconductor microcavities", Phys. Stat. Sol. B **242**, 2145-2356 (2005) and references therein.
- [15] I. Carusotto and C. Ciuti, Phys. Rev. Lett. **93**, 166401 (2004).
- [16] G. Dasbach *et al.*, Phys. Rev. B **64**, 201309(R) (2001).
- [17] O. El Daïf, A. Baas, T. Guillet, R. Idrissi-Katouni, J-L. Staehli, F. Morier-Genoud, and B. Deveaud, submitted.
- [18] I. Carusotto, Phys. Rev. A **63**, 023610 (2001).
- [19] A. Imamoglu *et al.*, Phys. Rev. Lett. **79**, 1467 (1997).
- [20] K.M. Bimbaum *et al.*, Nature **436** 87 (2005).
- [21] D.F. Walls and G.J. Milburn, *Quantum Optics* (Springer-Verlag, Berlin, 1994).